HHS Public Access

Author manuscript

Hepatology. Author manuscript; available in PMC 2020 May 01.

Published in final edited form as:

Hepatology. 2019 May ; 69(5): 1965–1982. doi:10.1002/hep.30525.

Adipocyte death preferentially induces liver injury and inflammation via the activation of CCR2+ macrophages and lipolysis

Seung-Jin Kim[1], **Dechun Feng**[1], **Adrien Guillot**[1], **Shen Dai**[2], **Fengming Liu**[2], **Seonghwan Hwang**[1], **Richard Parker**[1,3], **Wonhyo Seo**[1], **Yong He**[1], **Grzegorz Godlewski**[4], **Won-Il Jeong**[1,5], **Yuhong Lin**[6], **Xuebin Qin**[2], **George Kunos**[4], and **Bin Gao**[1,*]

[1]Laboratory of Liver Diseases, National Institute on Alcohol Abuse and Alcoholism, National Institutes of Health, Bethesda, MD 20892, USA

[2]Department of Neuroscience, School of Medicine, Temple University, Philadelphia, PA, USA

[3]NIHR Centre for Liver Research, University of Birmingham, UK

[4]Laboratory of Physiologic Studies, National Institute on Alcohol Abuse and Alcoholism, National Institutes of Health, Bethesda, MD 20892; USA

[5]Laboratory of Liver Research, Biomedical Science and Engineering Interdisciplinary Program, Korea Advanced Institute of Science and Technology (KAIST), Daejeon 34141, Republic of Korea

[6]Laboratory of Membrane Biochemistry and Biophysics, National Institute on Alcohol Abuse and Alcoholism, National Institutes of Health, Bethesda, MD 20892; USA

Abstract

Adipocyte death occurs under various physiopathological conditions, including obesity and alcohol drinking, and can trigger organ damage particularly in the liver, but the underlying mechanisms remain obscure. To explore these mechanisms, we developed a mouse model of inducible adipocyte death by overexpressing the human CD59 (hCD59) on adipocytes (adipocyte-specific *hCD59* transgenic mice). Injection of these mice with intermedilysin (ILY), which rapidly lyses hCD59 expressing cells exclusively by binding to the hCD59 but not mouse CD59, resulted in the acute selective death of adipocytes, adipose macrophage infiltration, and elevation of serum free fatty acid (FFA) levels. ILY injection also resulted in the secondary damage to multiple organs with the strongest injury observed in the liver, with inflammation and hepatic macrophage activation. Mechanistically, acute adipocyte death elevated epinephrine and norepinephrine levels and activated lipolysis pathways in adipose tissue in a $CCR2^+$ macrophage-dependent manner, which was followed by FFA release and lipotoxicity in the liver. Additionally, acute adipocyte

*Corresponding author: Bin Gao, M.D., Ph.D., Laboratory of Liver Diseases, NIAAA/NIH, 5625 Fishers Lane, Bethesda, MD 20892. Tel: 301-443-3998; bgao@mail.nih.gov.

Author contributions

SJK designed and conducted the experiments and wrote the paper; DF, AG, SH, RP, WS, YH, GG conducted the experiments; SD, FL prepared ILY; YL performed fatty acid composition analysis, WIJ, XQ, GK performed data analysis and edited the paper. BG supervised the whole project and wrote the paper.

Conflict of interest statement

The authors declare no competing interests.

death caused hepatic CCR2^{+} macrophage activation and infiltration, further exacerbating liver injury.

Conclusion: Adipocyte death predominantly induces liver injury and inflammation, which is probably due to the superior sensitivity of hepatocytes to lipotoxicity and the abundance of macrophages in the liver.

Keywords

FFA; lipotoxicity; organ damage; Kupffer cells; pancreatitis

Introduction:

Adipocyte death happens under various physiopathological conditions, including obesity,[1–3] alcohol consumption,[4] malignancy-associated weight loss,[5] pregnancy in obese women,[6] lipedema,[7] plastic surgery-associated adipose tissue ischemia,[8] insulin depletion,[9] consumption of conjugated linoleic acid,[10, 11] vitamin A supplementation,[12] etc. The link between adipocyte death and obesity-associated insulin resistance has been extensively investigated. [1, 2, 13] It is generally accepted now that adipose tissue expansion in obesity causes hypoxia and subsequent adipocyte death, which triggers chronic, low-grade inflammation, accumulation of extracellular matrix, and eventually insulin resistance.[1, 2, 13] However, the association of adipocyte death and the pathogenesis of organ damage is poorly understood. Several studies demonstrated that mitigation of adipocyte death by either global deletion of the *Bid* gene or adipocyte-specific deletion of the *Fas* gene ameliorated insulin resistance and fatty liver in high-fat diet fed mice; [14, 15] whereas adipocyte-specific deletion of the *Snap23* gene resulted in BAX-dependent adipocyte apoptosis, insulin resistance, and hepatic steatosis,[16] suggesting a link between adipocyte apoptosis and fatty liver development. Adipocyte death was also observed in chronically ethanol-fed mice, which is believed to be mediated via the induction of CYP2E1 activity and subsequent activation of Bid-mediated apoptosis and of complement.[4] Such adipocyte death likely induces adipose tissue inflammation, which may contribute to the pathogenesis of ethanol-induced liver injury.[4]

Although a link between adipocyte death and liver injury has been suggested by numerous studies, [4, 14, 17] the mechanisms by which adipocyte death triggers liver injury and damage to other organs remain unclear. The Scherer laboratory previously developed a mouse model of fat cell apoptosis through targeted activation of caspase 8, and by using this model they demonstrated that chronic induction of adipocyte death caused glucose intolerance, reduced systemic inflammatory responses and M2 macrophage recruitment in adipose tissues, and hepatic steatosis.[18, 19] The Konrad group reported that deletion of the *Fas* gene in adipocytes ameliorated adipose tissue inflammation and hepatic steatosis in high-fat diet-fed mice.[15] However, the effect of adipocyte death on liver injury and inflammation has not been characterized, and its effect on other organs was not reported. It is also difficult to observe the direct effect of adipocyte death on organ damage because chronic adipocyte death occurred in these models. In the current study, by crossing Cre-inducible floxed STOP-CD59 knock-in mice [20] with adiponectin Cre transgenic mice, we generated a unique model for acute adipocyte death in *AdiponectinCre^{+}ihCD59* transgenic mice

(*ihCD59*^{AdTG}), in which human complement regulator CD59 (hCD59) is specifically overexpressed in mouse adipocytes. Intermedilysin (ILY), a cytolytic pore-forming toxin that is secreted by Streptococcus intermedius, rapidly lyses human cells exclusively by binding to the human complement regulator CD59 (hCD59), but does not react with CD59 from non-primates.[21] Injection of ILY caused acute adipocyte death and crown-like structure (CLS) formation in adipose tissue in *ihCD59*^{AdTG} mice. Interestingly, acute adipocyte death also initiated the secondary damage to multiple organs with the profound injury and inflammation observed in the liver. Moreover, we found that acute adipocyte death directly releases free fatty acids (FFA) or activate the lipolysis pathway that subsequently induces production of FFAs, resulting in lipotoxicity and liver damage. Lipolysis in adipocytes is achieved by sequential action of adipose TG lipase (ATGL), hormone-sensitive lipase (HSL), and monoglyceride lipase, which hydrolyze triglycerides (TGs) to FFAs and glycerol.[22] Activation of β-adrenergic receptor by epinephrine (EPI) and norepinephrine (NE) is the best known classic factor to stimulate lipolysis in adipocytes via the activation of cAMP-dependent PKA and subsequent phosphorylation of HSL.[22] We demonstrated that acute adipocyte death caused elevation of plasma EPI and NE, activation of PKA and HSL in adipose tissues, and liver injury in a CCR2^{+} macrophage-dependent manner.

Material and Methods:

Mice.

The Cre-inducible human *CD59* knockin mice were generated as described previously.[20] Adiponectin-Cre mice (Stock No: 028020) were purchased from the Jax laboratory (Bar Harbor, ME). Female AdipoCre$^{+/-}$ mice and male *ihCD59*$^{flox/flox}$ mice were bred at the NIAAA FLAC facility to generate *AdipoCre*$^{+}$*ihCD59* (*ihCD59*^{AdTG}) and *AdipoCre*$^{-}$*ihCD59* (*ihCD59*) littermate controls. B6.129(Cg)-*Ccr2*$^{tm2.1Ifc}$/J mice (Stock No: 017586) in which the *Ccr2* coding region was replaced with a monomeric red fluorescent protein (RFP), were purchased from the Jax laboratory. *ihCD59*^{AdTG} mice were crossed with B6.129(Cg)-*Ccr2*$^{tm2.1Ifc}$/J to generate *ihCD59*^{AdTG}*Ccr2*$^{RFP+/-}$ mice that were used to label CCR2^{+} cells, and for several steps to generate *ihCD59*^{AdTG}*Ccr2*$^{RFP/RFP}$ mice in which *Ccr2* gene was disrupted (designed as *ihCD59*^{AdTG}*Ccr2*$^{-/-}$ double mutant mice). All mice were maintained in a specific pathogen-free facility and were cared for in accordance with National Institutes of Health guidelines. The study was approved by the National Institute on Alcohol Abuse and Alcoholism Animal Care and Use Committee.

ILY purification.

His-tagged recombinant ILY was purified as described previously.[20] The concentration and purity of ILY was determined by SDS-PAGE.

Immunofluorescence staining of CLEC-4F and IBA-1:

Liver tissues were fixed in 4% PFA, embedded in O.C.T compound and sectioned (10 μm). The sections were staining with anti-CLEC-4F (Cat: MAB2784, R&D systems), anti-IBA-1 antibody (Cat: 100369–764, VWR Corporate Headquarters, Radnor, PA). Fluorescent labeled secondary antibodies (Cell Signaling Technology) were used to visualize the primary

antibodies. The images were obtained by using LSM 710 confocal microscope (Zeiss, Thornwood, NY).

Measurement of serum epinephrine (EPI) and norepinephrine (NE).

Serum NE and EPI were measured with a commercial kit from Abnova (Catalog #KA1882). Samples were prepared and measured according to the manufacturer's instruction.

Statistical analysis.

The data are expressed as means ± S.E.M. (n=5–10 mice). To compare values obtained from two groups, the student t test was performed. Data from multiple groups were compared with one-way ANOVA followed by Turkey's post hoc test. Statistical significance was taken at the $P < 0.05$ level.

Many other methods are included in Supporting Materials including RT-PCR primer sequences in Supporting Table 1.

Results:

A model with acute adipocyte death and inflammation in ILY-treated *ihCD59*^{AdTG} mice

To study the pathological role of adipocyte death *in vivo*, we developed a model of acute adipocyte injury by using the ILY/*ihCD59* system. Briefly, floxedSTOP-hCD59 knock-in mice[20] were crossed with adiponectin Cre mice to generate adipocyte-specific hCD59 transgenic mice (*ihCD59*^{AdTG}) (Supporting Fig. S1A), in which hCD59 is specifically expressed in white adipose tissue (WAT) and brown adipose tissue (BAT) as confirmed by Western blot analysis (Supporting Fig. S1B), but not in the liver (Supporting Fig. S1C). Adiponectin Cre negative *ihCD59* knock-in mice, in which no hCD59 is expressed, were used as controls (*ihCD59*). *In vitro* experiments revealed that ILY treatment rapidly induced death of *hCD59*$^{+}$ adipocytes isolated from *ihCD59*^{AdTG} mice without affecting hCD59 ^{negative} adipocytes from *ihCD59* mice (Supporting Fig. S1D). To examine whether ILY kills adipocytes in adipose tissues from *ihCD59*^{AdTG} mice *in vivo*, we measured "Crown-like structure (CLS)", an indicator of adipocyte death formed by accumulation of macrophages around dead/injured adipocytes.[2, 23] Histological analysis of subcutaneous (Supporting Fig. S1E) and epididymal adipose tissue (Fig. 1A, Supporting Fig. S1F, showed an increase in CLS in *ihCD59*^{AdTG} after ILY injection compared with *ihCD59* mice. In addition, TUNEL assays revealed that TUNEL^{+} cells were highly increased in adipose tissue of *ihCD59*^{AdTG} mice after injection of ILY compared with *ihCD59* mice (Supporting Fig. S1G). Taken together, these findings suggest that injection of ILY induces adipocyte death in *ihCD59*^{AdTG} mice. H&E staining also showed histological changes of BAT with appearance of large lipid droplets in brown adipocytes of *ihCD59*^{AdTG} mice compared to *ihCD59* mice (Supporting Fig. S1F). Another evidence for adipocyte death is that serum levels of adiponectin, a major adipokine produced by adipocytes, was significantly reduced in ILY-treated *ihCD59*^{AdTG} mice compared to those in *ihCD59* mice (Fig. 1B). Serum levels of leptin and restistin were much lower compared to adiponectin; there were no differences in leptin between these two groups, and serum levels of restistin were even higher in ILY-treated *ihCD59*^{AdTG} mice verse *ihCD59* mice (Fig. 1B).

Since adipose tissue CLS is associated with phagocytic cell infiltration into adipose tissue, [24] we analyzed macrophage and neutrophil infiltration in adipose tissues. As illustrated in Supporting Fig. S1F, immunohistochemistry analyses revealed that ILY-treated *ihCD59*^{AdTG} mice had much higher number of F4/80^{+} macrophages and MPO^{+} neutrophils in adipose tissues compared to ILY-treated *ihCD59* mice. Furthermore, flow cytometric analysis of adipose tissues demonstrated that ILY injection elevated monocytes/macrophages (CD11b^{+}F4/80^{+}) and neutrophils (CD11b^{+}Gr-1^{+}) in the stromal vascular fraction (SVF) of *ihCD59*^{AdTG} mice compared to *ihCD59* (Fig. 1C). In addition, quantitative RT-PCR analyses revealed that expression of various inflammatory markers in adipose tissues was higher in ILY-treated *ihCD59*^{AdTG} mice than in ILY-treated *ihCD59* group (Fig. 1D). Interestingly, although adipose *Mcp-1* and *Tnf-a* mRNA levels were highly elevated in ILY-treated *ihCD59* mice, serum levels of MCP-1 and TNFα were not elevated (data not shown), suggesting that elevation of these pro-inflammatory cytokines is restricted locally in adipose tissues.

Acute adipocyte death induces secondary damage to multiple organs with the strongest liver injury associated with hepatic macrophage activation in ILY-treated *ihCD59*^{AdTG} mice

To determine the effects of acute adipocyte injury on organ damages, we measured a variety of parameters in the serum from ILY-treated *ihCD59*^{AdTG} mice. Table 1 shows that serum levels of ALT, AST, amylase, BUN, CK, glucose, lactate dehydrogenase were significantly elevated 2 hours post ILY injection in *ihCD59*^{AdTG} mice compared to those in ILY-treated *ihCD59* mice. Most of these parameters returned to the basal levels 8 hours post ILY injection except serum ALT, AST, and lactate dehydrogenase levels which were still highly elevated 8 hours post-ILY-treatment. These data suggest that ILY injection induces liver injury (as demonstrated by elevation of serum ALT, AST), pancreatic injury (as demonstrated by elevation of amylase), and possible damage to the kidneys (as demonstrated by elevation of BUN, CK etc) in *ihCD59*^{AdTG} mice. The effect of acute adipocyte death on pancreatic injury was further characterized. As illustrated in Supporting Fig. S2A, serum amylase and lipase levels were increased in *ihCD59*^{AdTG} compared with *ihCD59* mice after ILY injection. In addition, the number of TUNEL^{+} apoptotic acinar cells were significantly increased in pancreas from *ihCD59*^{AdTG} compared with *ihCD59* mice after ILY injection (Supporting Fig. S2B).

Of note, serum ALT and AST levels reached their peak 8 hours post ILY injection in *ihCD59*^{AdTG} mice (Fig. 2A), while injury markers for other organs returned to basal levels by that time. The significant liver injury post ILY injection was further demonstrated by elevation of caspase 3/7 activity (Fig. 2A) and cleaved caspase 3^{+} hepatocytes (Supporting Fig. S3A) in the liver in *ihCD59*^{AdTG} mice *verse ihCD59* mice.

The above data suggest that acute adipocyte death causes significant liver damage but only transient damage to other organs including the pancreas. Thus, we focused on and further characterized liver injury and inflammation. Immunostaining and quantitative RT-PCR analyses revealed that 8-hour post ILY injection there were greater number of F4/80^{+} macrophages, MPO^{+} neutrophils and TUNEL^{+} cells (Figs. 2B-C, Supporting Fig. S3B) and higher levels of hepatic pro-inflammatory markers (such as *Il-1b*) in ILY-treated

ihCD59^{AdTG} mice compared with ILY-treated *ihCD59* mice (Fig. 2D). One striking finding in ILY-treated *ihCD59*^{AdTG} mice was that hepatic macrophages were not only increased in number but also formed clusters and changed shapes, suggesting hepatic macrophage activation (Fig. 2B), and that such striking F4/80 macrophage activation was only observed in the liver but not in many other organs we examined (Supporting Fig. S4). In addition to increased hepatic inflammation, the number of circulating neutrophils and lymphocytes was higher in ILY-treated *ihCD59*^{AdTG} mice compared with ILY-treated *ihCD59* mice (Fig. 2E).

Because adipose death is associated with obesity, [1–3] we examined the effect of ILY induced adipocyte death in 2-month and 3-month HFD-fed *ihCD59*^{AdTG} mice. As illustrated in Supporting Fig. S5A, serum levels of ALT and FFA were significantly elevated in 2-month HFD-fed *ihCD59*^{AdTG} mice post ILY injection, but these levels are comparable to ILY-treated chow-fed *ihCD59*^{AdTG} mice as described in Figure 2. Surprisingly, serum ALT and FFA levels were not elevated in 3-month HFD-fed *ihCD59*^{AdTG} mice post ILY injection, this may be because 3-month HFD feeding already significantly caused adipocyte adipocyte and hepatocyte injury [1–3], which was reflected by high basal levels of serum FFAs and ALT, and higher number of F480^{+} CLS in adipose tissues in 3-month HFD-fed *ihCD59*^{AdTG} mice without ILY injection (Supporting Fig. S5A-B).

Acute adipocyte death elevates serum FFAs and induces adipose tissue lipolysis in ILY-treated *ihCD59*^{AdTG} mice as well as elevation of epinephrine (EPI) and norepinephrine (NE)

FFAs are known to directly induce hepatotoxicity,[25–27] so we wondered whether FFAs are elevated and these elevated FFAs contribute to liver injury in ILY-treated *ihCD59*^{AdTG} mice. As illustrated in Fig. 3A, serum levels of FFAs and glycerol were rapidly elevated with peak effects 2 hours post ILY injection. Furthermore, isolated adipose tissues from ILY-treated *ihCD59*^{AdTG} mice produced higher levels of FFAs than those from ILY-treated *ihCD59* mice (Fig. 3B). Elevated FFAs could be due to FFA release from injured adipocytes or due to elevated lipolysis in ILY-treated *ihCD59*^{AdTG} mice. Indeed, treatment of *ihCD59*^{AdTG} adipocytes *in vitro* with ILY, which induced adipocyte death, produced significant amounts of FFAs (Supporting Fig. S6A). To determine any differences in the compositions of FFAs from adipocyte death or lipolysis, we measured these compositions in the supernatant from ILY-treated *ihCD59*^{AdTG} adipocytes or lipolysis inducer forskolin-treated adipocytes. As illustrated in Supporting Fig. 6B, ILY-induced adipocyte death released similar compositions of FFAs as those generated from forskolin-induced lipolysis.

To further investigate whether lipolysis is involved FFA elevation in ILY-treated *ihCD59*^{AdTG} mice, we performed Western blot analysis to measure activation of lipolysis pathways such as phosphorylated PKA, which is known to activate HSL.[22] As illustrated in Fig. 3C, PKA and HSL phosphorylation were much higher in adipose tissues from ILY-treated *ihCD59*^{AdTG} mice compared with ILY-treated *ihCD59* mice. Furthermore, ATGL expression levels were also elevated in adipose tissues from *ihCD59*^{AdTG} mice after injection of ILY compared with *ihCD59* mice. In addition, mRNA expression of several lipolytic genes was significantly increased in *ihCD59*^{AdTG} after injection of ILY (Fig. 3D).

Activation of β-adrenergic receptors (ARs) by NE and EPI plays a key role in inducing lipolysis.[22] To examine the mechanisms underlying lipolysis in ILY-treated *ihCD59*^{AdTG}

mice, we measured plasma levels of NE and EPI, and adipose tissue expression of β-ARs. As illustrated in Fig. 3E, serum levels of NE and EPI, and expression of β1-AR and β3-AR in adipose tissues were much higher in *ihCD59*^{AdTG} mice compared to those in *ihCD59* mice post ILY injection.

Activation of lipolysis by the β-AR agonist isoproterenol induces strong lipolysis but weak liver injury and inflammation

The above data show that acute adipocyte death induces lipolysis and liver injury, suggesting that lipolysis-associated elevation of FFAs contributes liver injury in ILY-treated *ihCD59*^{AdTG} mice. To examine whether lipolysis-associated FFAs can directly induce liver injury, we treated mice with the β-AR agonist isoproterenol to induce lipolysis. As illustrated in Fig. 3F, injection of isoproterenol rapidly induced marked elevation of serum FFAs, indicating activation of lipolysis. Interestingly, isoproterenol injection also elevated serum ALT levels in mice although this elevation is much lower than that from ILY-treated *ihCD59*^{AdTG} mice as described in Fig. 2. Immunostaining analysis revealed that isoproterenol treatment increased MPO^{+} neutrophil infiltration and F4/80^{+} macrophage crown structure in adipose tissue (Supporting Fig. S7A). The number of MPO^{+} neutrophils but not F4/80^{+} macrophages in the liver was increased in isoproterenol-treated mice (Supporting Fig. S7B). Quantitative RT-PCR analyses show that expression of *Ly6G* and *Cd11b* was upregulated in adipose tissues post isoproterenol treatment (Supporting Fig. S7C). Hepatic expression of several pro-inflammatory markers and neutrophil markers (*Cd11b* and *Ly6g*) but not macrophage markers (*F4/80*) was upregulated post isoproterenol treatment (Supporting Fig. S7D).

Injection of FFAs (linoleic acid or oleic acid) induces liver injury independent of macrophages

To further test whether FFAs can directly induce liver injury, mice were treated with linoleic acid or oleic acid. As illustrated in Figs. 4A-B and supporting Table S2, injection of either linoleic acid or oleic acid markedly elevated serum levels of ALT, AST, and FFAs, as well elevated the level of circulating neutrophils. Hepatic expression of several chemokines, cytokines, and inflammatory markers was also elevated after injection of FFAs (Fig. 4C). Interestingly, most of these inflammatory markers are neutrophil-related (such as neutrophil marker *Ly6g*, chemokines for neutrophils: *E-selectin*, *Cxcl1, Cxcl2*), while markers for macrophages were not elevated (such as macrophage markers *Iba1, Cd68, F4/80*) (Fig. 4C). Immunohistochemistry analyses revealed that injection of linoleic acid or oleic acid increased MPO^{+} neutrophil infiltration but not F4/80^{+} macrophages (supporting Fig. S8), which may be due to FFA upregulation of hepatic CXCL1 (a key chemokine for neutrophils) that attract neutrophils.[28] Finally, deletion of macrophages by injection of clodronate-containing liposomes did not affect linoleic acid-induced elevation of serum ALT and AST and circulating leukocytes (Fig. 4D). The data in Fig. 4E confirmed that clodronate-induced deletion of macrophages resulted in marked downregulation of macrophage markers *Iba1, Cd68*, and *F4/80*; while expression of other inflammatory mediators was not markedly reduced except *Cxcl1*.

Depletion of macrophages/Kupffer cells prevents adipocyte death-induced liver injury and adipose tissue inflammation and lipolysis

The above data showed that F4/80^{+} macrophages were not only increased in numbers but also formed clusters, indicating hepatic macrophages/Kupffer cells are activated in ILY-treated *ihCD59*$^{\mathrm{AdTG}}$ mice. To determine the role of macrophages in hepatic injury in ILY-treated *ihCD59*$^{\mathrm{AdTG}}$ mice, we treated mice with clodronate-containing liposomes, which can deplete liver resident Kupffer cells and infiltrating macrophages. Immunostaining analyses in supporting Fig. S9A confirmed the complete depletion of F4/80^{+} cells in clodronate liposome-treated mice compared to empty liposome-treated mice. Interestingly, MPO^{+} cells were also depleted, which may be because depletion of macrophages abolished liver injury (see later results) and subsequently prevented MPO^{+} neutrophil infiltration. Quantitative RT-PCR revealed that hepatic *F4/80, Cd11b, IL-1b, IL-10* expression levels were significantly decreased following clodronate treatment in liver tissue of ILY-treated *ihCD59*$^{\mathrm{AdTG}}$ (Fig. 5A). Moreover, depletion of Kupffer cells/macrophages markedly reduced serum levels of ALT, AST, FFAs, and glycerol (Fig. 5B).

Fig. 5C shows that adipose expression of inflammatory markers (such as *F4/80, Tnfa,* and *Cd11b*) except *Mcp-1* was significantly downregulated in ILY-treated *ihCD59*$^{\mathrm{AdTG}}$ mice after clodronate-induced macrophage depletion, suggesting that clodronate injection also depletes macrophages in adipose tissues, and upregulation of *Mcp-1* is independent of macrophages. Furthermore, protein expression of activated lipolytic pathways such as pPKA, pHSL, and ATGL was much lower in adipose tissues from macrophage-depleted groups compared to those from vehicle control groups (Fig. 5D). In addition, expression of HSL, ATGL, and perilipin mRNAs in adipose tissues was lower in ILY-treated *ihCD59*$^{\mathrm{AdTG}}$ mice with macrophage depletion than in those without macrophage depletion (Fig. 5E). Interestingly, depletion of macrophages markedly reduced serum epinephrine in ILY-treated *ihCD59*$^{\mathrm{AdTG}}$ mice (Fig. 5E).

Genetic deletion of the *Ccr2* gene ameliorates liver injury and inflammation in ILY-treated *ihCD59*$^{\mathrm{AdTG}}$ mice

Clodronate treatment depleted both resident liver Kupffer cells and infiltrating macrophages. To further distinguish the roles of liver resident Kupffer cells and infiltrating macrophages, we characterized these two populations in the liver by performing double staining with IBA-1 and CLEC-4F. Kupffer cells express both IBA-1 and CLEC-4F, while infiltrating macrophages only express IBA-1.[29] As illustrated in Fig. 6A, both ILY-treated *ihCD59*$^{\mathrm{AdTG}}$ and *ihCD59* mice contained high number of IBA-1^{+}CLEC-4F^{+} Kupffer cells in the liver. Interestingly, CLEC-4F$^{\mathrm{negative}}$ IBA-1^{+} infiltrating macrophage clusters were only observed in the liver from the ILY-treated *ihCD59*$^{\mathrm{AdTG}}$ mice, suggesting significant number of infiltrating macrophages in the liver. To further define infiltrating macrophages express CCR2, we generated *ihCD59*$^{\mathrm{AdTG}}$*Ccr2*$^{\mathrm{RFP+/-}}$ mice, in which CCR2^{+} monocytes are labelled with RFP protein. As illustrated in Fig. 6B, immunohistochemistry analyses of RFP protein revealed that ILY injection markedly elevated CCR2$^{\mathrm{RFP+}}$ macrophages in adipose tissues and the liver from *ihCD59*$^{\mathrm{AdTG}}$*Ccr2*$^{\mathrm{RFP+/-}}$ mice with significant number of CCR2$^{\mathrm{RFP+}}$ clusters in the liver compared to WT mice. Flow cytometric analyses further confirmed that

the number of CCR2^{RFP+} cells was increased in the liver from ILY-treated *ihCD59*^{AdTG}*Ccr2*$^{RFP+/-}$ mice *vs. Ccr2*$^{RFP+/-}$ mice (Fig. 6B).

Flow cytometric analyses demonstrated that hepatic CD11b^{+}F4/80^{low} infiltrating macrophages from ILY-treated *ihCD59*^{AdTG} mice were significantly elevated (10.8% in *ihCD59*^{AdTG} *vs.* 5.57% in *ihCD59*) (Fig. 6C) and displayed an activation phenotype such as lower levels of CD62L (downregulation of CD62L indicates activation) compared to those from ILY-treated *ihCD59* mice (Fig. 6D). Moreover, quantitative RT-PCR analyses demonstrated that expression of M1 macrophage marker *iNos* was highly upregulated in mononuclear cells from the liver and peripheral blood but not from adipose tissues (Fig. 6E). Next, we performed flow cytometric analysis to determine the cell types with upregulated iNOS and found that iNOS protein was markedly increased in CD45^{+} CCR2^{+}CD11b^{+}Ly6G^{-} infiltration macrophages from the liver (Fig. 6F) but not in CCR2^{+} cells from peripheral blood (supporting Fig. S9B) in ILY-treated *ihCD59*^{AdTG} mice.

To define whether CCR2, which is important for tissue macrophage infiltration associated with obesity,[30–32] is required for CCR2^{+} macrophage infiltration and whether it plays a role in acute adipocyte death-induced liver injury, we generated double mutant *ihCD59*^{AdTG}*Ccr2*$^{-/-}$ mice. As illustrated in Fig. 7A-C, the number of F4/80^{+} macrophages and MPO^{+} neutrophils in adipose tissues and the liver was markedly lower in ILY-treated *ihCD59*^{AdTG}*Ccr2*$^{-/-}$ mice compared to those in ILY-treated *ihCD59*^{AdTG} mice. Interestingly, significant clustering of F4/80^{+} cells was observed in the liver from ILY-treated *ihCD59*^{AdTG} mice but such clusters were not observed in ILY-treated *ihCD59*^{AdTG}*Ccr2*$^{-/-}$ mice (Fig. 7A). Quantitative RT-PCR confirmed that expression of many inflammatory mediators in adipose tissues was reduced as a result of *Ccr2* deletion (Supporting Fig. S10A). Interestingly, in the liver only *Ly6g* (a marker for neutrophils) and *Ccr2* were reduced in ILY-treated *ihCD59*^{AdTG}*Ccr2*$^{-/-}$ mice *vs. ihCD59*^{AdTG} mice; whereas expression of several other inflammatory markers was comparable between these two groups (Supporting Fig. S10A).

Finally, as illustrated in Fig. 7D, serum ALT levels and circulating neutrophil numbers were lower in *ihCD59*^{AdTG}*Ccr2*$^{-/-}$ mice compared to *ihCD59*^{AdTG} mice post ILY injection. Serum levels of EPI in *ihCD59*^{AdTG}*Ccr2*$^{-/-}$ mice were also lower compared to those in *ihCD59*^{AdTG} mice post ILY injection, whereas serum NE levels were comparable between these two groups. Expression of lipolysis-related genes (eg. *Hsl, Atgl, perilipin, AR1, and AR2*) in adipose tissues was reduced in ILY-treated *ihCD59*^{AdTG}*Ccr2*$^{-/-}$ mice compared to ILY-treated *ihCD59*^{AdTG} mice (Supporting Fig. S10B). Serum FFA levels were markedly lower in ILY-treated in *ihCD59*^{AdTG}*Ccr2*$^{-/-}$ mice than those in ILY-treated *ihCD59*^{AdTG} mice (Supporting Fig. S10C).

The above data suggest that CCR2 is required for liver injury and inflammation in ILY-treated *ihCD59*^{AdTG} mice. Next we examined whether CCR2 also contributes to liver injury induced by isoproterenol or FFAs. As illustrated in Supporting Fig. S11, injection of isoproterenol or linoleic acid had comparable levels of serum ALT and hepatic expression of most inflammatory genes in WT and *Ccr2*$^{-/-}$ mice. As expected, hepatic expression of *Ccr2* gene was not detected in *Ccr2*$^{-/-}$ mice. Interestingly, the number of circulating neutrophils

and hepatic expression of *Ly6g* (the neutrophil marker) were lower in isoproterenol-treated *Ccr2*$^{-/-}$ mice compared to WT mice but were comparable between linoleic acid-treated *Ccr2*$^{-/-}$ and WT mice. Taken together, these data suggest that CCR2 does not contribute to liver injury induced by isoproterenol or linoleic acid, and that CCR2 plays a role in elevating neutrophils after isoproterenol treatment but not after linoleic acid treatment.

Discussion

Although adipocyte death occurs under various physiopathological conditions, its impact on organ damage remains obscure. Several previous studies generated mouse models of chronic adipocyte death and investigated how chronic adipocyte death affects insulin resistance and hepatic steatosis; [14–16] however, the effects of adipocyte death on organ damage and inflammation have not been explored. In the current study, we demonstrated a link between adipocyte death and damage to multiple organs, most notably to the liver, by using a mouse model of selective adipocyte death model induced by ILY treatment. Injection of ILY to *ihCD59*^{AdTG} mice rapidly induced multiple organ damage (such as elevation of serum ALT, AST, amylase, BUN, CK etc) that peaked at two hours post injection, which correlates with the rapid elevation of serum FFAs, suggesting that these multiple organ damages are due to FFA-mediated lipotoxicity.[33] Interestingly, these parameters except ALT and AST returned to normal levels by 8 hours post injection, which was the time when serum ALT and AST levels peaked. Such prolonged elevation of serum ALT and AST may be attributed to strong hepatic macrophage infiltration and activation, as expression of the macrophage marker F4/80 as well as macrophage clusters was markedly elevated in the liver but not in other organs of these mice. The mechanisms by which acute adipocyte death causes liver injury and inflammation were further investigated and are summarized in Fig. 7E, which depicts how adipocyte death likely initiates macrophage activation and liver injury.

Adipocyte death has been linked to chronic adipose tissue inflammation and macrophage infiltration, but the exact mechanisms are not fully understood. By taking advantage of an acute adipocyte death model of ILY-treated *ihCD59*^{AdTG} mice, we observed macrophage infiltration as early as two hours post ILY injection, which correlates with marked (12-fold) upregulation of *Mcp-1* in adipose tissues at this time point. Given the important role of MCP-1 in inducing macrophage recruitment in adipose tissue and the liver,[34–36] such rapid elevation of MCP-1 is likely responsible for macrophage infiltration after adipocyte death. Although both adipocytes and macrophages produce MCP-1,[34] our findings that deletion of macrophages only slightly reduced *Mcp-1* expression in adipose tissues in ILY-treated *ihCD59*^{AdTG} mice suggests that elevation of *Mcp-1* is primarily derived from adipocytes. Moreover, we demonstrated for the first time that adipocyte death-induced macrophage activation triggers the lipolysis pathway in adipose tissues. First, serum FFAs and glycerols as well as adipose tissue FFAs were highly elevated after adipocyte death in ILY-treated *ihCD59*^{AdTG} mice. Second, adipocyte death markedly upregulated several lipolysis-related genes including p-PKA, p-HSL, and ATGL proteins, as well as *Hsl, Atgl, perilipin*, and *Dagt1* mRNAs in adipose tissues. Third, serum levels of EPI and NE, the two primary stimulators of lipolysis,[22] were significantly elevated in *ihCD59*^{AdTG} mice post ILY injection. Finally, depletion of macrophages by injection of clodronate liposomes prevented elevation of NE and EPI and the subsequent activation of lipolysis in ILY-treated

ihCD59^{AdTG} mice. Collectively, our data suggest that infiltrating macrophages associated with adipocyte death contribute to the elevation of NE and EPI and the subsequent activation of lipolysis. However, the mechanisms by which macrophage activation results in elevated NE and EPI levels are not clear. Future studies are required to define whether infiltrating macrophages directly produce catecholamines or indirectly affect sympathetic nerve to produce catecholamines in our models.

Another interesting finding from our study is that injection of the β-AR agonist isoproterenol, a classic lipolysis activator, caused much stronger lipolysis activation but less liver injury than ILY injection in *ihCD59*^{AdTG} mice. This is probably because in addition to lipolysis-related lipotoxicity, other factor(s) such as macrophage activation may also attribute to adipocyte death-associated liver injury. Indeed, there are much more infiltrating macrophages and macrophage clusters in the liver from ILY-treated *ihCD59*^{AdTG} mice compared to those in isoproterenol- or FFA-treated mice. Depletion of macrophages or the *Ccr2* gene (which encodes a key chemokine receptor for macrophage infiltration) abolished liver injury in ILY-treated *ihCD59*^{AdTG} mice but did not affect isoproterenol- or FFA-induced liver damage, suggesting both macrophage activation in adipose tissue and FFA-mediated lipotoxicity contribute to liver injury in ILY-treated *ihCD59*^{AdTG} mice. The next obvious question was how do adipocyte death-associated macrophages trigger liver injury. A recent study revealed that activated macrophages in adipose tissues promoted neutrophil recruitment and macrophage activation in the liver in mouse models of NASH.[37, 38] Therefore, it is plausible that adipocyte death-associated macrophage activation promotes liver injury by stimulating neutrophil recruitment and subsequently worsening lipolysis-mediated lipotoxicity and liver injury. Indeed, ILY treatment induced marked neutrophil infiltration in *ihCD59*^{AdTG} mice, such infiltration was blunted after macrophage/Kupffer cell depletion or deletion of the *Ccr2* gene. Moreover, the infiltrating macrophages in the liver from ILY-treated *ihCD59*^{AdTG} mice had elevated expression of iNOS, which may also promote liver injury by inducing nitric oxide production.[39] Finally, the infiltrating macrophages can produce a variety of proinflammatory cytokines such as TNF-α and IL-1β that can induce hepatocyte damage.[40–43]

Clinical significance of this study:

Obesity is well known to be associated with adipocyte death and inflammation in humans,[1, 2] and a recent study in patients with NASH reported that adipose tissue inflammation correlated positively with the severity of NASH, based on serum ALT levels and NAFLD activity score.[44] In particular, the proportions of $CD11C^+CD206^+$ and $CCR2^+$ macrophages in adipose tissues were highly elevated in NASH patients compared to healthy controls and to obese patients with fatty liver.[44] A more recent study reported that $CCR2^+$ macrophages were also markedly elevated in the livers from NASH patients and correlated with NASH severity.[31] However, the mechanistic underpinning of adipocyte death/inflammation and liver injury was not addressed by these studies and remain obscure. The present preclinical findings demonstrate that adipocyte death can trigger adipose tissue macrophage infiltration and lipolysis and subsequent liver damage via the activation of $CCR2^+$ macrophages. These findings should stimulate further studies of adipocyte death and

lipolysis in NASH patients, which may support a novel therapeutic strategy of blocking adipocyte death as a way to alleviate NASH.

Supplementary Material

Refer to Web version on PubMed Central for supplementary material.

Acknowledgements

This work was supported by the intramural program of NIAAA, NIH (BG, GK), and R01 HL130233, HL141132 (XQ).

Abbreviations:

ALT	alanine aminotransferase
AST	aspartate aminotransferase
AT	adipose tissue
ATGL	adipose TG lipase
BAT	brown adipose tissue
CLS	crown like structure
CLEF-4F	C-Type Lectin Domain Family 4 Member F
d	day(s)
FFAs	free fatty acids
h	hour(s)
hCD59	human complement regulator CD59
HFD	high-fat diet
HSL	hormone-sensitive lipase
IBA1	Ionized calcium binding adaptor molecule 1
IHC	immuno-histochemistry
ILY	Intermedilysin
MPO	myeloperoxidase
PCR	polymerase chain reaction
TG	triglyceride
WAT	white adipose tissue

References

1. Sun K, Kusminski CM, Scherer PE. Adipose tissue remodeling and obesity. J Clin Invest 2011;121:2094–2101. [PubMed: 21633177]
2. Strissel KJ, Stancheva Z, Miyoshi H, Perfield JW 2nd, DeFuria J, Jick Z, et al. Adipocyte death, adipose tissue remodeling, and obesity complications. Diabetes 2007;56:2910–2918. [PubMed: 17848624]
3. Murano I, Barbatelli G, Parisani V, Latini C, Muzzonigro G, Castellucci M, Cinti S. Dead adipocytes, detected as crown-like structures, are prevalent in visceral fat depots of genetically obese mice. J Lipid Res 2008;49:1562–1568. [PubMed: 18390487]
4. Sebastian BM, Roychowdhury S, Tang H, Hillian AD, Feldstein AE, Stahl GL, et al. Identification of a cytochrome P4502E1/Bid/C1q-dependent axis mediating inflammation in adipose tissue after chronic ethanol feeding to mice. J Biol Chem 2011;286:35989–35997. [PubMed: 21856753]
5. Prins JB, Walker NI, Winterford CM, Cameron DP. Human adipocyte apoptosis occurs in malignancy. Biochem Biophys Res Commun 1994;205:625–630. [PubMed: 7999091]
6. Haghiac M, Vora NL, Basu S, Johnson KL, Presley L, Bianchi DW, Hauguel-de Mouzon S. Increased death of adipose cells, a path to release cell-free DNA into systemic circulation of obese women. Obesity (Silver Spring) 2012;20:2213–2219. [PubMed: 22836687]
7. Suga H, Araki J, Aoi N, Kato H, Higashino T, Yoshimura K. Adipose tissue remodeling in lipedema: adipocyte death and concurrent regeneration. J Cutan Pathol 2009;36:1293–1298. [PubMed: 19281484]
8. Suga H, Eto H, Aoi N, Kato H, Araki J, Doi K, et al. Adipose tissue remodeling under ischemia: death of adipocytes and activation of stem/progenitor cells. Plast Reconstr Surg 2010;126:1911–1923. [PubMed: 21124131]
9. Loftus TM, Kuhajda FP, Lane MD. Insulin depletion leads to adipose-specific cell death in obese but not lean mice. Proc Natl Acad Sci U S A 1998;95:14168–14172. [PubMed: 9826672]
10. Miner JL, Cederberg CA, Nielsen MK, Chen X, Baile CA. Conjugated linoleic acid (CLA), body fat, and apoptosis. Obes Res 2001;9:129–134. [PubMed: 11316347]
11. Hargrave KM, Li C, Meyer BJ, Kachman SD, Hartzell DL, Della-Fera MA, et al. Adipose depletion and apoptosis induced by trans-10, cis-12 conjugated linoleic Acid in mice. Obes Res 2002;10:1284–1290. [PubMed: 12490673]
12. Jeyakumar SM, Vajreswari A, Sesikeran B, Giridharan NV. Vitamin A supplementation induces adipose tissue loss through apoptosis in lean but not in obese rats of the WNIN/Ob strain. J Mol Endocrinol 2005;35:391–398. [PubMed: 16216918]
13. McNelis JC, Olefsky JM. Macrophages, immunity, and metabolic disease. Immunity 2014;41:36–48. [PubMed: 25035952]
14. Alkhouri N, Gornicka A, Berk MP, Thapaliya S, Dixon LJ, Kashyap S, et al. Adipocyte apoptosis, a link between obesity, insulin resistance, and hepatic steatosis. J Biol Chem 2010;285:3428–3438. [PubMed: 19940134]
15. Wueest S, Rapold RA, Schumann DM, Rytka JM, Schildknecht A, Nov O, et al. Deletion of Fas in adipocytes relieves adipose tissue inflammation and hepatic manifestations of obesity in mice. J Clin Invest 2010;120:191–202. [PubMed: 19955656]
16. Feng D, Amgalan D, Singh R, Wei J, Wen J, Wei TP, et al. SNAP23 regulates BAX-dependent adipocyte programmed cell death independently of canonical macroautophagy. J Clin Invest 2018;128:3941–3956. [PubMed: 30102258]
17. Parker R, Kim SJ, Gao B. Alcohol, adipose tissue and liver disease: mechanistic links and clinical considerations. Nat Rev Gastroenterol Hepatol 2018;15:50–59. [PubMed: 28930290]
18. Pajvani UB, Trujillo ME, Combs TP, Iyengar P, Jelicks L, Roth KA, et al. Fat apoptosis through targeted activation of caspase 8: a new mouse model of inducible and reversible lipoatrophy. Nat Med 2005;11:797–803. [PubMed: 15965483]
19. Fischer-Posovszky P, Wang QA, Asterholm IW, Rutkowski JM, Scherer PE. Targeted deletion of adipocytes by apoptosis leads to adipose tissue recruitment of alternatively activated M2 macrophages. Endocrinology 2011;152:3074–3081. [PubMed: 21693678]

20. Feng D, Dai S, Liu F, Ohtake Y, Zhou Z, Wang H, et al. Cre-inducible human CD59 mediates rapid cell ablation after intermedilysin administration. J Clin Invest 2016;126:2321–2333. [PubMed: 27159394]
21. Giddings KS, Zhao J, Sims PJ, Tweten RK. Human CD59 is a receptor for the cholesterol-dependent cytolysin intermedilysin. Nat Struct Mol Biol 2004;11:1173–1178. [PubMed: 15543155]
22. Fruhbeck G, Mendez-Gimenez L, Fernandez-Formoso JA, Fernandez S, Rodriguez A. Regulation of adipocyte lipolysis. Nutr Res Rev 2014;27:63–93. [PubMed: 24872083]
23. Cinti S, Mitchell G, Barbatelli G, Murano I, Ceresi E, Faloia E, et al. Adipocyte death defines macrophage localization and function in adipose tissue of obese mice and humans. J Lipid Res 2005;46:2347–2355. [PubMed: 16150820]
24. Lumeng CN, Deyoung SM, Bodzin JL, Saltiel AR. Increased inflammatory properties of adipose tissue macrophages recruited during diet-induced obesity. Diabetes 2007;56:16–23. [PubMed: 17192460]
25. Malhi H, Gores GJ. Molecular mechanisms of lipotoxicity in nonalcoholic fatty liver disease. Semin Liver Dis 2008;28:360–369. [PubMed: 18956292]
26. Alkhouri N, Dixon LJ, Feldstein AE. Lipotoxicity in nonalcoholic fatty liver disease: not all lipids are created equal. Expert Rev Gastroenterol Hepatol 2009;3:445–451. [PubMed: 19673631]
27. Li S, Dou X, Ning H, Song Q, Wei W, Zhang X, et al. Sirtuin 3 acts as a negative regulator of autophagy dictating hepatocyte susceptibility to lipotoxicity. Hepatology 2017;66:936–952. [PubMed: 28437863]
28. Wang W, Xu MJ, Cai Y, Zhou Z, Cao H, Mukhopadhyay P, et al. Inflammation is independent of steatosis in a murine model of steatohepatitis. Hepatology 2017;66:108–123. [PubMed: 28220523]
29. Scott CL, Zheng F, De Baetselier P, Martens L, Saeys Y, De Prijck S, et al. Bone marrow-derived monocytes give rise to self-renewing and fully differentiated Kupffer cells. Nat Commun 2016;7:10321. [PubMed: 26813785]
30. Weisberg SP, Hunter D, Huber R, Lemieux J, Slaymaker S, Vaddi K, et al. CCR2 modulates inflammatory and metabolic effects of high-fat feeding. J Clin Invest 2006;116:115–124. [PubMed: 16341265]
31. Krenkel O, Puengel T, Govaere O, Abdallah AT, Mossanen JC, Kohlhepp M, et al. Therapeutic inhibition of inflammatory monocyte recruitment reduces steatohepatitis and liver fibrosis. Hepatology 2018;67:1270–1283. [PubMed: 28940700]
32. Parker R, Weston CJ, Miao Z, Corbett C, Armstrong MJ, Ertl L, et al. CC chemokine receptor 2 promotes recruitment of myeloid cells associated with insulin resistance in nonalcoholic fatty liver disease. Am J Physiol Gastrointest Liver Physiol 2018;314:G483–G493. [PubMed: 29420066]
33. Savary S, Trompier D, Andreoletti P, Le Borgne F, Demarquoy J, Lizard G. Fatty acids - induced lipotoxicity and inflammation. Curr Drug Metab 2012;13:1358–1370. [PubMed: 22978392]
34. Kanda H, Tateya S, Tamori Y, Kotani K, Hiasa K, Kitazawa R, et al. MCP-1 contributes to macrophage infiltration into adipose tissue, insulin resistance, and hepatic steatosis in obesity. J Clin Invest 2006;116:1494–1505. [PubMed: 16691291]
35. Baeck C, Wehr A, Karlmark KR, Heymann F, Vucur M, Gassler N, et al. Pharmacological inhibition of the chemokine CCL2 (MCP-1) diminishes liver macrophage infiltration and steatohepatitis in chronic hepatic injury. Gut 2012;61:416–426. [PubMed: 21813474]
36. Raeman R, Anania FA. Therapy for steatohepatitis: Do macrophages hold the clue? Hepatology 2018;67:1204–1206. [PubMed: 29091293]
37. Bijnen M, Josefs T, Cuijpers I, Maalsen CJ, van de Gaar J, Vroomen M, et al. Adipose tissue macrophages induce hepatic neutrophil recruitment and macrophage accumulation in mice. Gut 2018;67:1317–1327. [PubMed: 29074725]
38. Pernes G, Lancaster GI, Murphy AJ. Take me to the liver: adipose tissue macrophages coordinate hepatic neutrophil recruitment. Gut 2018;67:1204–1206. [PubMed: 29298875]
39. Chen T, Zamora R, Zuckerbraun B, Billiar TR. Role of nitric oxide in liver injury. Curr Mol Med 2003;3:519–526. [PubMed: 14527083]

40. McGettigan B, McMahan R, Orlicky D, Burchill M, Danhorn T, Francis P, et al. Dietary Lipids Differentially Shape NASH Progression and the Transcriptome of Kupffer Cells and Infiltrating Macrophages. Hepatology 2018.

41. Zhang J, Zhang Q, Lou Y, Fu Q, Chen Q, Wei T, et al. Hypoxia-inducible factor-1alpha/interleukin-1beta signaling enhances hepatoma epithelial-mesenchymal transition through macrophages in a hypoxic-inflammatory microenvironment. Hepatology 2018;67:1872–1889. [PubMed: 29171040]

42. Tacke F Targeting hepatic macrophages to treat liver diseases. J Hepatol 2017;66:1300–1312. [PubMed: 28267621]

43. Ambade A, Lowe P, Kodys K, Catalano D, Gyongyosi B, Cho Y, et al. Pharmacological inhibition of CCR2/5 signaling prevents and reverses alcohol-induced liver damage, steatosis and inflammation in mice. Hepatology 2018.

44. du Plessis J, van Pelt J, Korf H, Mathieu C, van der Schueren B, Lannoo M, et al. Association of Adipose Tissue Inflammation With Histologic Severity of Nonalcoholic Fatty Liver Disease. Gastroenterology 2015;149:635–648 e614. [PubMed: 26028579]

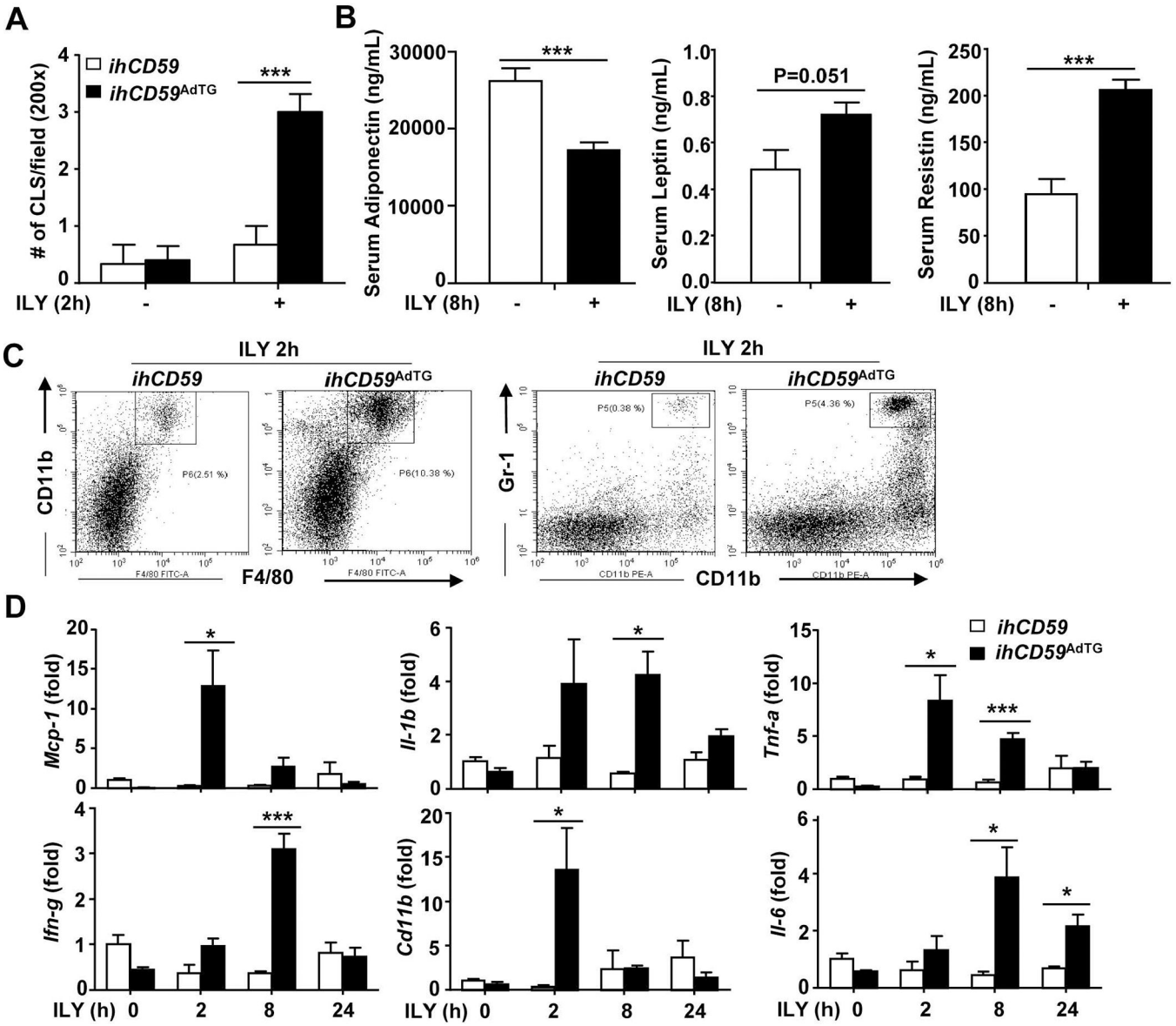

Figure 1. ILY injection induces adipocyte death and inflammation in *ihCD59*^{AdTG} mice.

ihCD59^{AdTG} and their littermate control (*ihCD59*) mice were treated with ILY for various time points as indicated. (A) The number of crown-like structure (CLS) number per field for H&E stained white adipose tissues was counted. (B) Serum levels of adipokines were measured. (C) Flow cytometric analysis of immune cells in adipose tissues. (D) RT-qPCR analysis of inflammatory markers in adipose tissues. Values represent means ± S.E.M. (n=5–8). **P*<0.05, ****P*<0.001

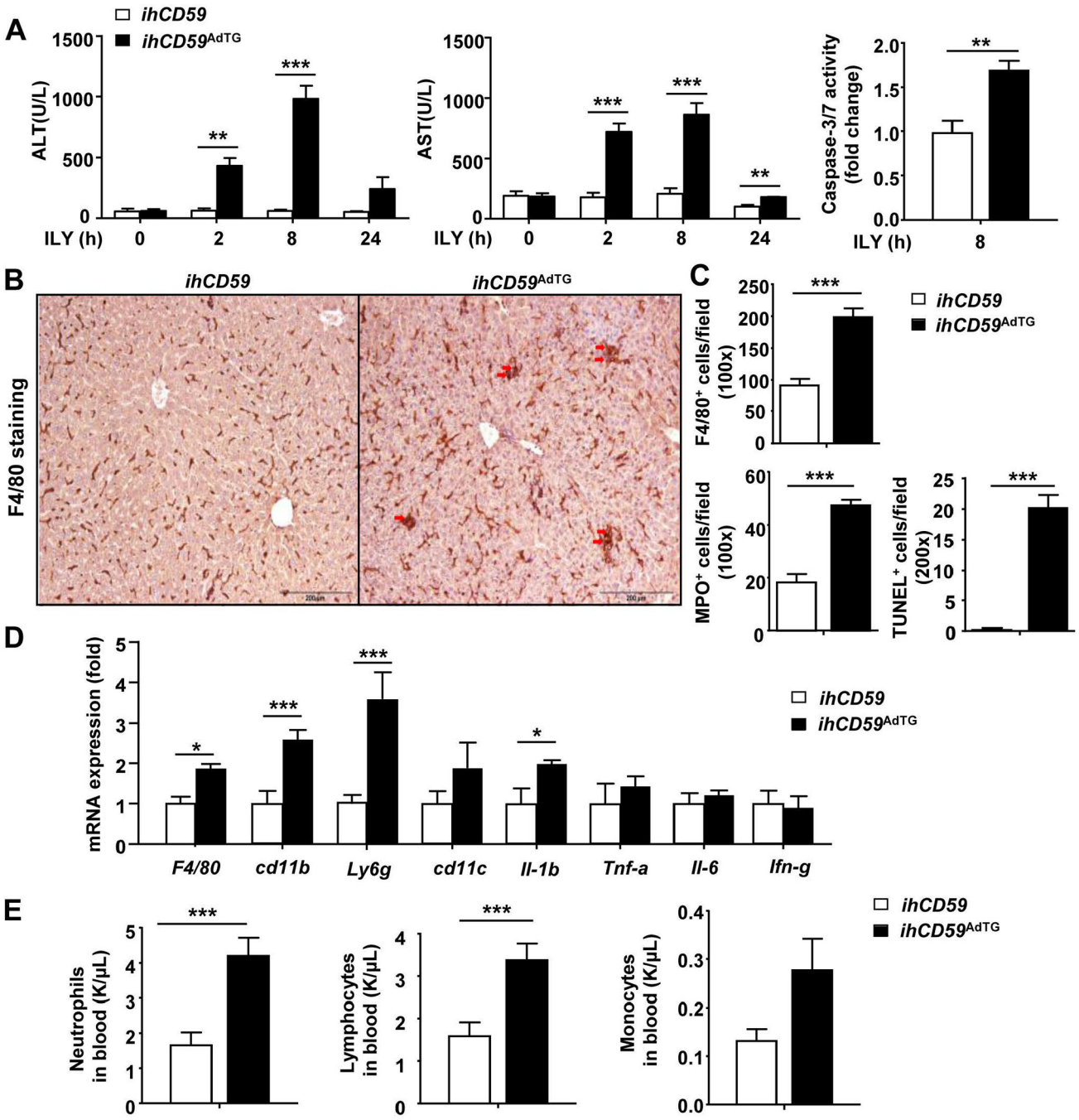

Figure 2. Acute adipocyte death causes liver injury and inflammation in ILY-treated *ihCD59*^{AdTG} mice.

ihCD59^{AdTG} and their littermate control (*ihCD59*) mice were treated with ILY for various time periods. Liver tissues and serum samples were collected for analyses. (A) Serum ALT and AST levels. Liver caspase 3/7 activity was measured and is shown in the right. (B) Representative F4/80 staining of liver tissues 8 hours post ILY injection (n=5). (C) Quantitation of F4/80, MPO and TUNEL positive cells from panel B (n=5). (D) RT-qPCR analysis of inflammatory markers in liver tissues 8 hours post ILY injection (n=4). (E)

Number of peripheral blood cells (n=7). Values represent means ± S.E.M. *P<0.05, **P<0.01, ***P<0.001

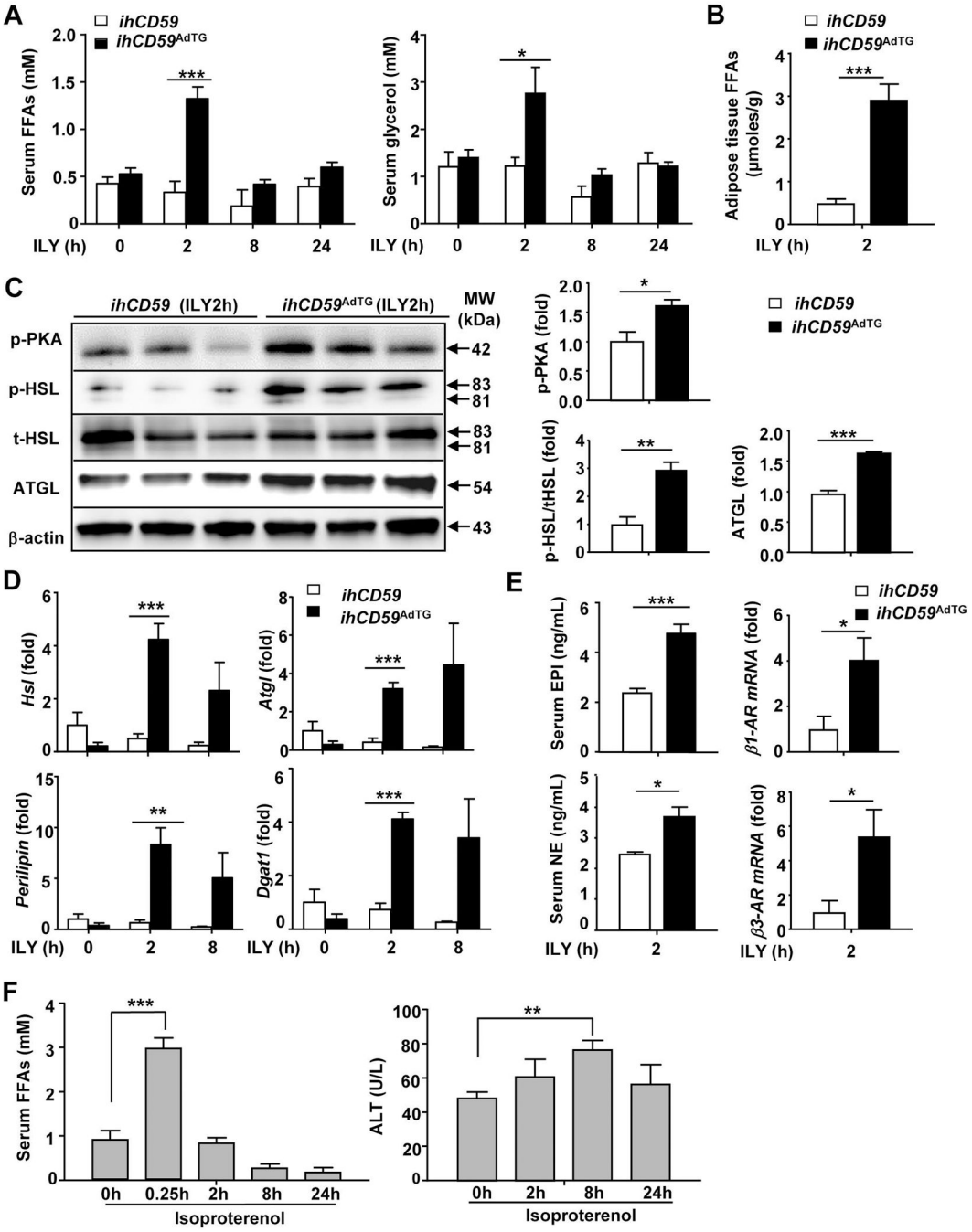

Figure 3. ILY injection induces lipolysis in *ihCD59*^{AdTG} mice: Evidence lipolysis weakly contributes to liver injury.

(A-E) *ihCD59*^{AdTG} and their littermate control (*ihCD59)* mice were treated with ILY for various time points. (A) Serum FFA and glycerol levels. (B) Adipose tissue explants were isolated from 2-hour ILY-treated mice and cultured *in vitro*, and release of FFAs in the supernatant was measured. (C, D) Western blot (C) and RT-qPCR (D) analyses of lipolytic genes. (E) Serum EPI, NE levels and RT-qPCR analyses of β-AR genes. **(F)** Isoproterenol injection induces strong lipolysis but weak liver injury. C57BL/6J mice were treated with

isoproterenol for various time points. Serum FFAs and ALT levels were measured. Values represent means ± S.E.M. (n=5–8). *P<0.05, **P<0.01, ***P<0.001

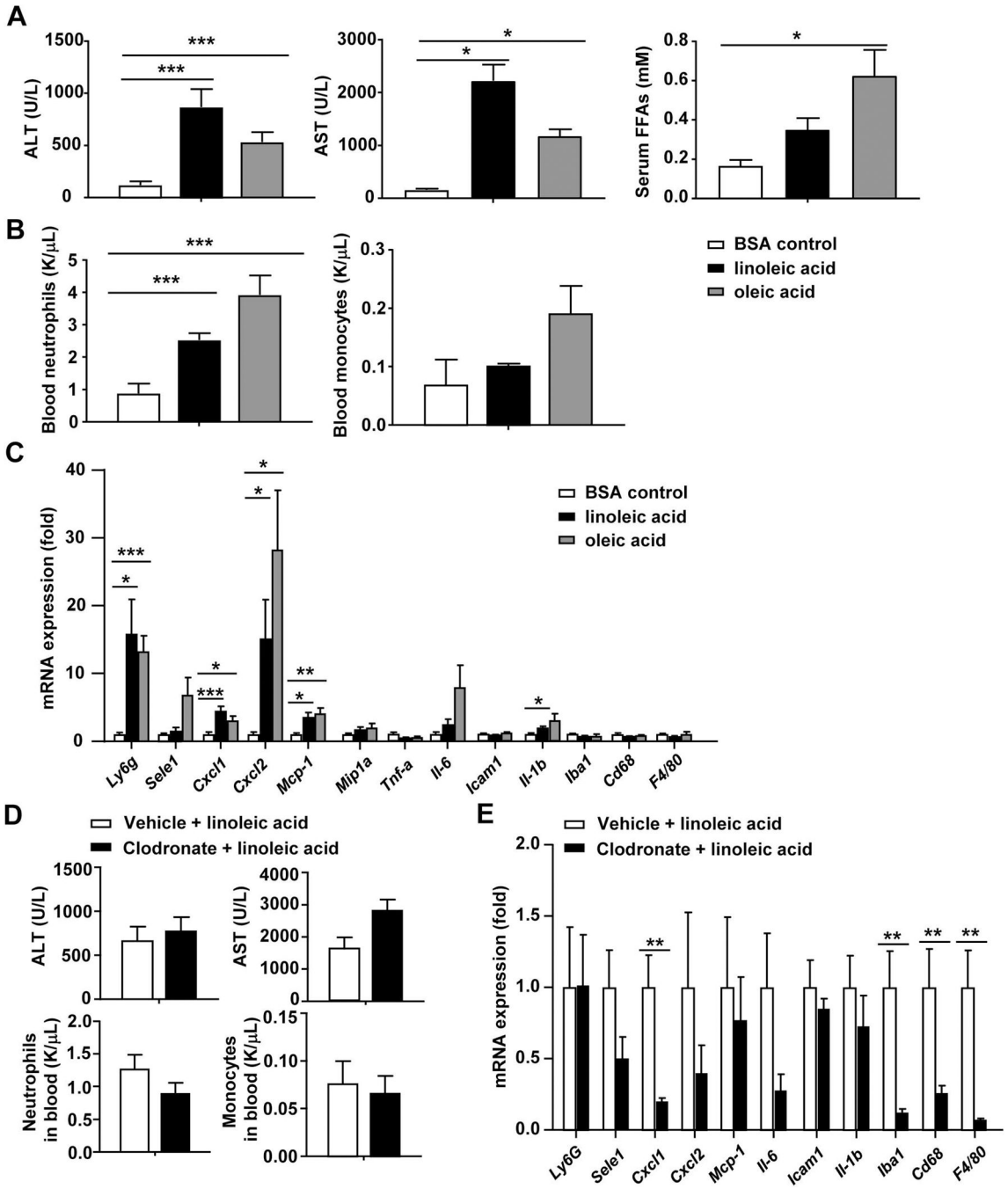

Figure 4. FFA injection induces liver injury independent of macrophages.

(A-C) Linoleic acid and oleic acid were conjugated with BSA at a 4:5 volume ratio before injection. C57BL/6J mice were intraperitoneally injected with BSA, the oleic acid or linoleic acid (1 mg/g body weight) for 6 hours. (A) Serum ALT, AST and FFA levels were measured. (B) Number of peripheral blood cells were counted. (C) Pro-inflammatory cytokine mRNA levels in the liver were measured by RT-qPCR. (D, E) C57BL/6 mice were injected with clodronate liposomes or liposomes for 24 hours, followed by injection of linoleic acid for 6 hours. Serum ALT, AST and number of peripheral blood cells were measured as shown in

panel D. Hepatic pro-inflammatory cytokines were measured by qRT-PCR as shown in panel E. Values represent means ± S.E.M. (n=5–6). *P<0.05, **P<0.01, ***P<0.001

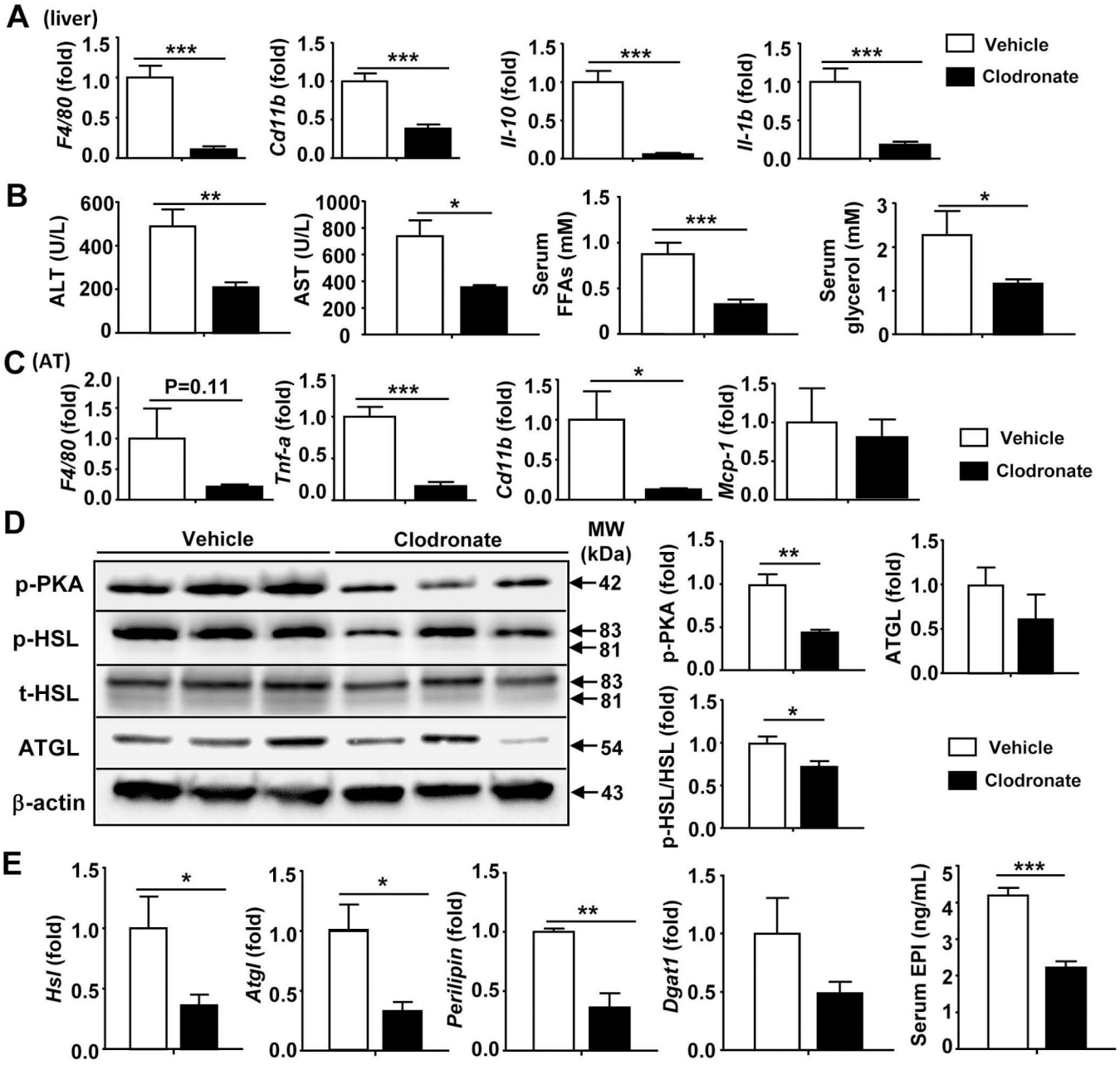

Figure 5. Macrophage depletion attenuates ILY induced liver inflammation and injury in *ihCD59*^{AdTG} mice.

ihCD59^{AdTG} mice were injected with Liposomal Clodronate for 24 hours to deplete Kupffer cells/macrophages, and then injected with ILY. Mice were sacrificed 2 hours post ILY injection. (A) RT-qPCR analyses of macrophage markers and cytokines in liver tissues. (B) Serum levels of ALT, AST, FFAs, and glycerol. (C) RT-qPCR analyses of pro-inflammatory mediators in adipose tissues. (D) Western blot analyses of adipose tissues. (E) RT-qPCR analyses of lipolytic genes in adipose tissues, and serum EPI levels from ILY-treated *ihCD59*^{AdTG} mice with or without macrophage depletion. Values represent means ± S.E.M. (n=5–6). **P*<0.05, ***P*<0.01, ****P*<0.001

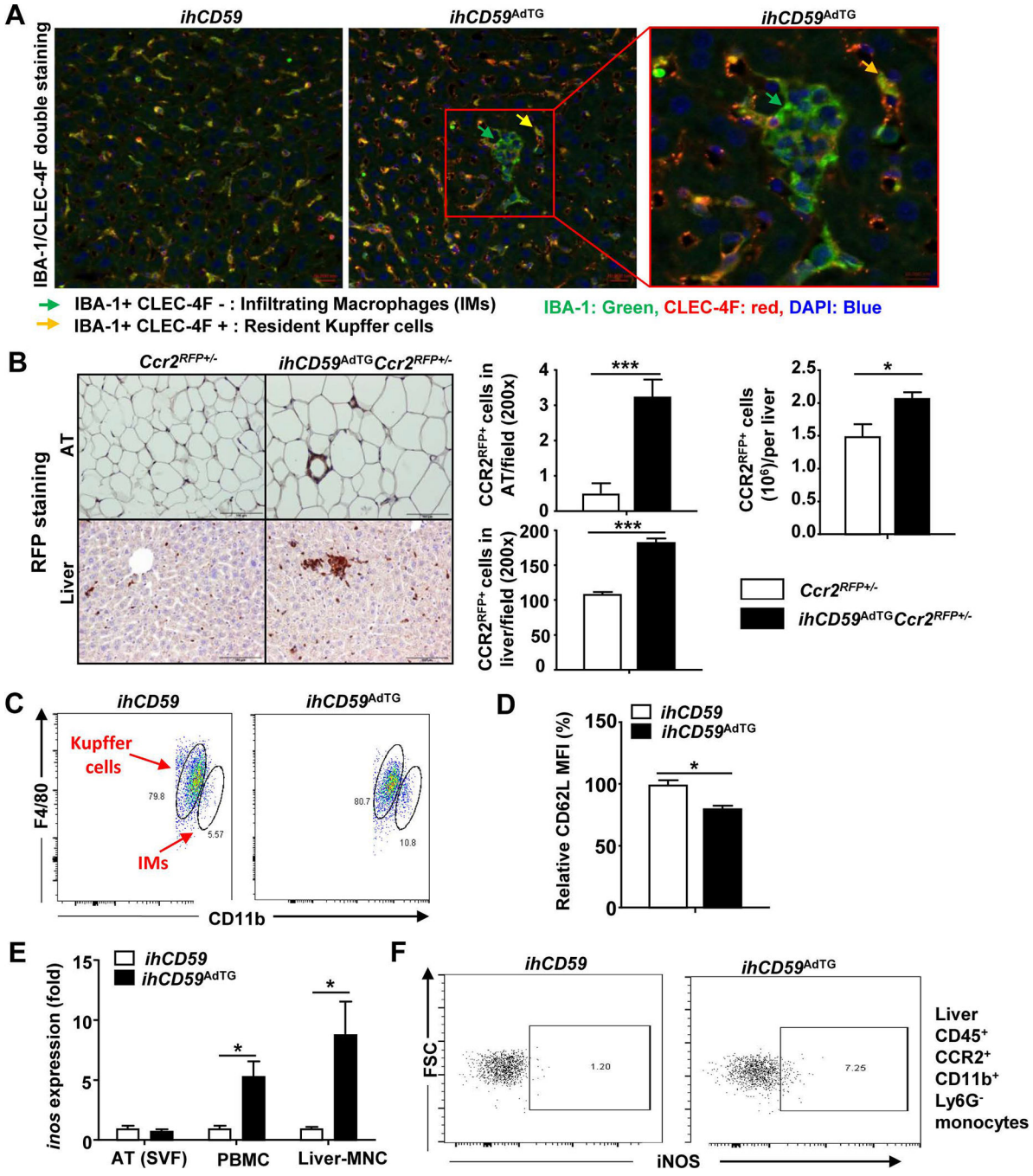

Figure 6. Accumulation and clustering of infiltrating macrophages (IMs) in the liver in ILY-treated *ihCD59*^{AdTG} mice.

(A) Immunofluorescence with anti-IBA-1 (green) and anti-CLEC-4F (red) antibody in liver tissues from 8-hour ILY-treated *ihCD59* and *ihCD59*^{AdTG} mice. (B) Immunohistochemistry with anti-RFP antibody in liver and AT tissues from 8-hour ILY-treated *Ccr2*$^{RFP+/-}$ and *ihCD59*^{AdTG}*Ccr2*$^{RFP+/-}$ mice, and the number of CCR2^{RFP+} cells/per field was quantified. The number of CCR2^{RFP+} cells/per liver was quantified by flow cytometric analysis and is shown in the right. (C) *ihCD59* and *ihCD59*^{AdTG} mice were treated with ILY for 8 hours. Flow cytometric analysis of Kupffer cells and infiltrating macrophages (IMs) in liver and is

shown. (D) Flow cytometric analysis of CD62L expression in infiltrating macrophages and the CD62L density was quantified. (E) RT-qPCR analysis of iNOS in AT-SVF, PBMC and liver-MNC. (F) Flow cytometric analysis of iNOS in liver $CD45^{+}CCR2^{+}CD11b^{+}Ly6G^{-}$ cells. Values represent means ± S.E.M. (n=5–6). *P<0.05, ***P<0.001. AT: adipose tissue; IM: infiltrating macrophages; MNC: mononuclear cells; PBMC: peripheral blood mononuclear cell; SVF: stromal-vascular fraction.

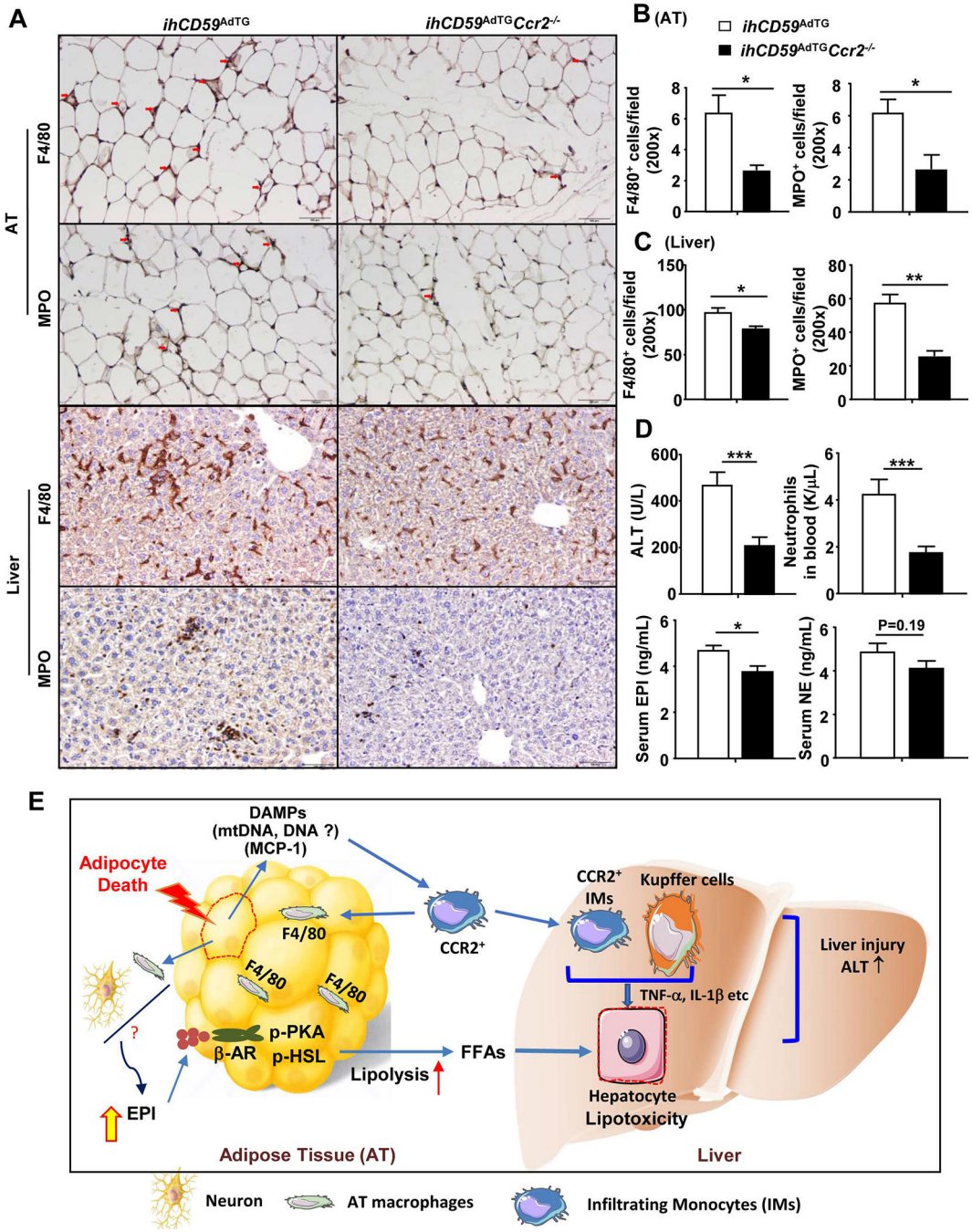

Figure 7. An additional deletion of the *Ccr2* gene reduces macrophage and neutrophil infiltration in adipose tissue (AT) and liver, and subsequently ameliorates liver injury in ILY-treated *ihCD59*^{AdTG} mice.

ihCD59^{AdTG} and *ihCD59*^{AdTG}*Ccr2*$^{-/-}$ mice were treated with ILY for 8 hours, adipose, liver, and serum samples were collected for analyses. (A) Immunohistochemistry analysis of F4/80 and MPO. (B, C) F4/80^{+} and MPO^{+} cells/per field were counted. (D) Serum ALT, EPI, NE and circulating neutrophils were determined. Values represent means ± S.E.M. (n=7). **P*<0.05, ***P*<0.01, ****P*<0.001. AT: adipose tissue. (**E**) A model depicting how adipocyte death triggers adipose inflammation and subsequently causes liver injury and

inflammation. Adipocyte death causes $CCR2^+$ macrophage infiltration and activation in adipose tissues. These activated $CCR2^+$ macrophages contribute to elevation of epinephrine and norepinephrine, and subsequently induce lipolysis and fatty acid release, and lipotoxicity in the liver. Additionally, acute adipocyte death also causes hepatic $CCR2^+$ macrophage infiltration, activation and clustering, further exacerbating liver injury.

Table. 1

Serum biochemistry profiles of ILY-treated *ihCD59* and *ihCD59*^{AdTG} mice

Variables	*ihCD59* (ILY 2h)	*ihCD59* ^{AdTG}(ILY2h)	p Value*	*ihCD59* (ILY 8h)	*ihCD59*^{AdTG}(ILY 8h)	p Value*
Alkaline Phosphatase (U/L)	201.50 ±45.20	194.50 ±30.42	0.90	172.00117.57	206.00142.49	0.49
ALT (U/L)	41.50 ±6.95	283.50 ±21.31	0.0001	50.00114.76	495.50148.64	0.000
AST (U/L)	151.00 ±25.98	380.50 ±81.77	0.05	160.50130.34	328.00122.14	0.004
Albumin (g/dL)	3.65 ±0.10	3.00 ±0.08	0.002	3.1510.17	3.2510.17	0.69
Cholesterol (mg/dL)	69.50 ±4.57	50.50 ±3.50	0.02	86.5016.95	71.5016.29	0.16
Triglyceride(mg/dL	83.00 ±5.51	108.50 ±23.21	0.33	77.00119.64	54.0016.48	0.31
Sodium (mmol/L)	319.00 ±1.29	319.50 ±1.26	0.79	319.5010.96	318.5010.50	0.39
Potassium (mmol/L)	7.30 ±0.33	9.55 ±1.07	0.09	7.7510.41	6.6010.22	0.05
Chloride (mmol/L)	258.50 ±0.96	261.50 ±0.50	0.05	260.0012.45	260.5010.50	0.85
Calcium (mmol/L)	2.34 ±0.03	2.19±0.06	0.07	2.2410.04	2.2510.01	0.71
Magnesium(mmol/L)	1.34 ±0.05	1.50 ±0.11	0.24	1.2010.08	1.1110.05	0.31
Phosphorus (mg/dL)	23.45 ±0.42	24.95±0.82	0.15	22.3510.28	21.2010.47	0.08
Amylase (U/L)	2713.50 ±241.50	8491.00 ±2262.00	0.05	3490.501705.40	7407.5012543.00	0.19
BUN (mg/dL)	20.00 ±0.82	43.00 ±3.00	0.0005	25.5014.79	27.5012.06	0.71
Creatinine (mg/dL)	0.20	0.25 ±0.05	0.36	0.20	0.20	-
CK (CKA5) (U/L)	1227.00 ±239.40	3295.50 ±814.40	0.05	950.001145.50	1607.001332.60	0.12
Glucose (mg/dL)	126.00 ±6.58	159.50 ±5.97	0.01	138.00115.10	149.5019.43	0.54
LactateDehydrogenase (U/L)	464.00 ±70.78	1784.00 ±151.60	0.0002	393.00188.78	1186.501265.50	0.05
Protein (g/dL)	4.80 ±0.16	4.1010.21	0.05	4.6510.25	4.4010.22	0.48
Uric Acid (mg/dL)	2.70 ±0.30	3.7010.66	0.22	2.7010.24	2.2010.08	0.09
Bilirubin (mg/dL)	<0.2	<0.2	-	<0.2	<0.2	-

ihCD59^{AdTG} and their littermate control *ihCD59* mice were treated with ILY for 2 hours or 8 hours. Serum was collected for measurement of various parameters. Data are presented as mean ±S.E.M. p Value* in this column was obtained from t-test analysis of two groups of *ihCD59* and *ihCD59*^{AdTG}.

*p Value in this column was obtained from t-test analysis of two groups of *ihCD59* and *ihCD59*^{AdTG}.